REPORT R-726 APRIL, 1976 UILU-ENG 76-2214

CSL COORDINATED SCIENCE LABORATORY

MULTITARGET SPUTTERING USING DECOUPLED PLASMA

C.E. WICKERSHAM
J.E. GREENE

APPROVED FOR PUBLIC RELEASE. DISTRIBUTION UNLIMITED.

UNIVERSITY OF ILLINOIS – URBANA, ILLINOIS

UNCLASSIFIED

SECURITY CLASSIFICATION OF THIS PAGE *(When Data Entered)*

REPORT DOCUMENTATION PAGE		READ INSTRUCTIONS BEFORE COMPLETING FORM
1. REPORT NUMBER	2. GOVT ACCESSION NO.	3. RECIPIENT'S CATALOG NUMBER
4. TITLE *(and Subtitle)* MULTITARGET SPUTTERING USING DECOUPLED PLASMAS		5. TYPE OF REPORT & PERIOD COVERED Technical Report
		6. PERFORMING ORG. REPORT NUMBER R-726; UILU-ENG 76-2214
7. AUTHOR(s) C. E. Wickersham and J. E. Greene		8. CONTRACT OR GRANT NUMBER(s) DAAB-07-72-C-0259
9. PERFORMING ORGANIZATION NAME AND ADDRESS Coordinated Science Laboratory University of Illinois at Urbana-Champaign Urbana, Illinois 61801		10. PROGRAM ELEMENT, PROJECT, TASK AREA & WORK UNIT NUMBERS
11. CONTROLLING OFFICE NAME AND ADDRESS Joint Services Electronics Program		12. REPORT DATE April, 1976
		13. NUMBER OF PAGES 26
14. MONITORING AGENCY NAME & ADDRESS *(if different from Controlling Office)*		15. SECURITY CLASS. *(of this report)* UNCLASSIFIED
		15a. DECLASSIFICATION/DOWNGRADING SCHEDULE

16. DISTRIBUTION STATEMENT *(of this Report)*

Approved for public release; distribution unlimited

17. DISTRIBUTION STATEMENT *(of the abstract entered in Block 20, if different from Report)*

18. SUPPLEMENTARY NOTES

19. KEY WORDS *(Continue on reverse side if necessary and identify by block number)*

Semiconductors
Sputtering
Thin Films

20. ABSTRACT *(Continue on reverse side if necessary and identify by block number)*

A model is derived for quantitatively predicting the chemical composition and thickness distributions of multielement films deposited by decoupled-plasma multitarget RF sputtering in which the substrates rotate at a variable rate through separate glow discharges. The model directly accounts for deposition variables such as target voltages, sputtering pressure, substrate rotation radius, rotation rate, and target-substrate separation distance. The effects of substrate heating and/or biasing are also considered. Predicted film thickness distributions were found to agree very well with experimental

DD FORM 1 JAN 73 1473 EDITION OF 1 NOV 65 IS OBSOLETE

SECURITY CLASSIFICATION OF THIS PAGE *(When Data Entered)*

SECURITY CLASSIFICATION OF THIS PAGE(*When Data Entered*)

20. ABSTRACT (continued)

results in which β back-scattering was used to measure the thickness of films deposited from InSb and GaSb targets on both stationary and rotating substrates. Using deposition parameters determined from the model presented in this paper, it is possible to grow single phase stoichiometric alloy films of any desired composition. In addition, intercalated films with layer thicknesses of less than 100 Å and films which are chemically graded in the lateral and in-depth directions can be grown.

SECURITY CLASSIFICATION OF THIS PAGE(*When Data Entered*)

UILU-ENG 76-2214

MULTITARGET SPUTTERING USING DECOUPLED PLASMAS

by

C. E. Wickersham and J. E. Greene

This work was supported in part by the Joint Services Electronics Program (U.S. Army, U.S. Navy and U.S. Air Force) under Contract DAAB-07-72-C-0259.

Reproduction in whole or in part is permitted for any purpose of the United States Government.

Approved for public release. Distribution unlimited.

ABSTRACT

A model is derived for quantitatively predicting the chemical composition and thickness distributions of multielement films deposited by decoupled-plasma multitarget RF sputtering in which the substrates rotate at a variable rate through separate glow discharges. The model directly accounts for deposition variables such as target voltages, sputtering pressure, substrate rotation radius, rotation rate, and target-substrate separation distance. The effects of substrate heating and/or biasing are also considered. Predicted film thickness distributions were found to agree very well with experimental results in which β backscattering was used to measure the thickness of films deposited from InSb and GaSb targets on both stationary and rotating substrates. Using deposition parameters determined from the model presented in this paper, it is possible to grow single phase stoichiometric alloy films of any desired composition. In addition, intercalated films with layer thicknesses of less than 100 Å and films which are chemically graded in the lateral and in-depth directions can be grown.

I. INTRODUCTION

Sputter deposition of multicomponent thin films has received a great deal of attention in the literature during the last 15 years. Applications include semiconductor device contacts [1], thin film thermistors [2], hard wear-resistant coatings [3], ferroelectric alloys [4], superconducting alloys [5], etc. At least three different sputtering techniques have been reported. These include: alloy sputtering [6] in which a single homogeneous target is used; plasma-coupled multitarget sputtering [7] in which two or more separately powered targets are sputtered in the same discharge; and cosputtering [8] from a single non-homogeneous target such as, for example, a target disc in which one half is material A and the other half material B.

All of the above techniques suffer from severe limitations for thin film growth studies. Alloy sputtering requires a separate target for each desired film composition and specification of target composition requires prior knowledge of elemental sticking probabilities if elevated temperature or reverse bias are to be applied to the substrate during film growth. Plasma-coupled multitarget sputtering does not allow independent control over target sputtering rates since a change at one target is manifested through the discharge as an uncontrolled change at the other targets. Both plasma-coupled multitarget sputtering and cosputtering result in large lateral non-uniformities in the chemical composition and film thickness within the substrate plane. In cosputtering these differences are accentuated when individual target sections have large differences in secondary electron emission coefficients [9] or

sputtering yields. This latter case can lead to target surface cone formation [10,11] and non-steady state sputtering [12]. Under more ideal conditions Hanak et al. [13] have shown that the distribution of film thickness and chemical composition can be predicted a-priori for a given geometry and he has used this technique to study alloy systems [14].

Recently, Corsi [15] and Greene, Wickersham, and Zilko [16,17], have used plasma decoupled multitarget sputtering to grow ternary semiconducting alloys. Greene et al. have shown that $In_xGa_{1-x}Sb$ thin films could be grown at any desired composition ranging from $x = 0$ to $x = 1$ from pure InSb and GaSb targets. Each target is sputtered independently and the substrates rotate at a controlled rate through each plasma. Furthermore, it was shown that films with any desired chemistry ranging from homogeneous to chemically stepped or chemically graded junctions could be grown by a systematic change in deposition variables. Good control over both film composition and thickness was easily maintained using this technique.

In the present paper we present a model for predicting a-priori the chemical composition of films deposited from multiple plasma-decoupled targets as a function of deposition variables such as target diameters, target to substrate plane separations, substrate rotation rate, rotation radius, target voltages, and sputtering pressure. The effects of substrate temperature and bias are also considered and an expression which predicts the film thickness at any point on the substrate plane is derived. Measurements of film thickness distributions are included and shown to be in good agreement with predicted values.

II. THEORETICAL MODEL FOR PREDICTING FILM THICKNESS AND CHEMICAL COMPOSITION DISTRIBUTIONS USING DECOUPLED MULTITARGET SPUTTERING

The chemical composition of a homogeneous film deposited by multitarget sputtering at any point (x',y') on a rotating substrate can be determined from the following simple equation

$$\text{vol. \% } j = 100 \left[\lambda_j(x',y') / \sum_{i=1}^{N} \lambda_i(x',y') \right] \tag{1}$$

where λ_j is the film thickness deposited per pass under target j. Thus the problem becomes one of calculating the film thickness distribution per target pass for each target as a function of substrate rotation rate (ω), rotation radius (ρ), target bias (V), target radius (s), target-electrode separation (h), and sputtering pressure (P). A schematic diagram which defines the terms to be used in this paper and shows the geometric relationship between the jth target and the substrate is given in Figure 1. The effects of substrate heating and biasing are not treated directly in this section but will be considered in section IV.

We have shown previously that the stationary substrate sputtering rate for several different semiconducting [16,17], oxide [18], and metallic targets [19] under typical RF sputtering conditions can be expressed as

$$R(x=0,\ y=0) = R_o V^{b(p)} \tag{2}$$

where R_o is the rate coefficient which is a function of the target material, sputtering pressure, substrate temperature, target radius, and target substrate separation. The exponent b typically varies from 1.5 to 2.5 depending on target material and sputtering pressure. At normal RF

sputtering pressures the distribution of material deposited on a stationary substrate can be described by von Hipple's equation [20] which assumes a cosine sputter ejection distribution and no scattering in the discharge. Experimental results confirming this equation will be presented in the next section. In terms of the co-ordinate system shown in Figure 1, the normalized von Hipple distribution function can be written as

$$D_j(x,y) = \left[\frac{s^2+h^2}{2s^2}\right]\left[1 - \frac{h^2 + (x^2+y^2) - s^2}{\{[h^2-(x^2+y^2)+s^2]^2 + 4h^2(x^2+y^2)]\}^{1/2}}\right]$$

$$= \left[\frac{s^2+h^2}{2s^2}\right] F(x,y) \quad (3)$$

Combining equations (2) and (3) we obtain

$$R(x,y) = R_o V^b \left(\frac{s^2+h^2}{2s^2}\right) F(x,y)$$

$$= \frac{1}{2}\,\Gamma\, F(x,y) \quad (4)$$

where Γ is independent of system geometry and is defined as

$$\Gamma = R(0,0)\left(\frac{s^2+h^2}{s^2}\right) \quad (5)$$

Physically, Γ is the target sputtering rate for a given V and P, or the deposition rate as $h \to 0$ in the absence of substrate heating and bias.

For the case of a rotating substrate, the film thickness per target pass can be written as

$$\lambda_j(x',y') = \frac{1}{\omega}\,\eta_j(0,0)\, G_j(x',y')\, R_j(0,0) \quad (6)$$

where $R_j(0,0)$ is just the stationary substrate deposition rate at the point (x = 0, y = 0) as defined in Figure 1. The term $\eta_j(0,0)$ is the ratio of the deposition rate when the substrate is rotating to that when it is stationary

$$\eta_j(0,0) = R'_j(0,0)/R_j(0,0) \tag{7}$$

$\eta_j(0,0)$ can be estimated from the ratio of the full width at half maximum of the stationary substrate film thickness distribution to the circumference of the circle swept out by the center of the rotating substrate. The term $G_j(x',y')$ in equation (6) also depends on system geometry factors such as target diameter and electrode separation and is the normalized stationary substrate distribution function transformed into the rotating coordinate system.

The equations to transform a stationary coordinate system referenced to the target to a substrate coordinate system rotating at velocity v can be obtained from Figure 1 where

$$\frac{dy}{dt} = v \cos \theta = 2\pi\omega \sqrt{\xi^2 - y^2} \tag{8}$$

and

$$\frac{dx}{dt} = v \sin \theta = 2\pi\omega y \ . \tag{9}$$

ξ is the radius vector in the substrate plane from the rotation axis to the point (x',y') in the rotating coordinate system. Equations (8) and (9) can be solved for x and y using the following boundary conditions: at t = 0, $y = \xi \sin \theta_o$ and at $t = \theta_o/2\pi\omega$, x = x'. The transformation equations thus become

$$y = \xi \sin(2\pi\omega t - \theta_o) \tag{10}$$

and

$$x = x' - \xi[1 + \cos(2\pi\omega t - \theta_o)] \ . \tag{11}$$

Equations (10) and (11) can now be used to transform the stationary distribution function $F_j(x,y)$ into the rotating substrate distribution function $F'_j(x',y',t)$. The geometric factor which accounts for off-origin distribution is then defined by

$$G_j(x',y') = \frac{\int_o^{T_j(x',y')} F'_j(x',y't)\, dt}{\int_o^{T_j(0,0)} F'_j(0,0,t)\, dt} \tag{12}$$

where the integral in the denominator normalizes the distribution to the origin.

The integration limit $T_j(x',y')$ in equation (12) represents the total time that the point (x',y') on the substrate is exposed to the target. Thus $T_j(x',y')$ is the path length swept out by the point (x',y') in the plasma divided by the velocity, or

$$T_j(x',y') = \frac{2\theta_{oj}\xi}{2\pi\omega\xi} = \frac{\theta_{oj}}{\pi\omega} \ . \tag{13}$$

The angle θ_{oj} can be obtained by geometry from Figure 1 and is given by

$$\theta_{oj} = \cos^{-1}\left[\frac{\rho^2 + \xi^2 - r_{oj}^{\ 2}}{2\rho\xi}\right] \tag{14}$$

where r_{oj} is the stationary distribution truncation radius beyond which it is assumed that the deposition rate is zero.

Once the rotating substrate thickness distribution of each component in the film is determined, the film composition may be found by combining equations (1), (5), (6), and (12):

$$\text{vol. \% } j = \frac{\Gamma_j \eta_j \left[\frac{s_j^2}{s_j^2 + h^2}\right] \frac{\int_o^{T_j(x',y')} F_j'(x',y't)\, dt}{\int_o^{T_i(0,0)} F_j'(0,0,t)\, dt}}{\sum_{i=1}^{m} \Gamma_i \eta_i \left[\frac{s_i^2}{s_i^2 + h^2}\right] \frac{\int_o^{T_i(0,0)} F_i'(x',y't)\, dt}{\int_o^{T_i(0,0)} F_i'(0,0,t)\, dt}} \qquad (15)$$

where all parameters are known. For a given set of deposition variables in which von Hipple's distribution function, equation (3), does not apply, the actual measured stationary substrate distribution function F(x,y) must be used. However, as will be demonstrated in the next section, von Hipple's equation accurately describes the film thickness distribution over a wide range of RF sputtering deposition conditions.

Figure 2 shows a set of computer calculated rotating substrate thickness distributions for a rotation radius of 20 cm, a target-substrate separation of 5 cm, and target radii of 2.5 cm, 5.0 cm, and 7.5 cm. The von Hipple stationary target distribution was used in these calculations and r_{oj} was chosen such that deposition was cut off at the radius at which von Hipple's distribution function reaches 0.5% of its maximum value. For the deposition variables given in Figure 2, the truncation radius r_{oj} varied from 19.38 cm for the 2.5 cm radius target to 25.79 cm for the 7.5 cm radius target. The asymmetry of the distributions and the absolute

magnitude of the deposited film thickness at ($x' = 0$, $y' = 0$) increases with increasing target radius. The curves in Figure 2 are normalized to the hypothetical value of film thickness one would obtain with no electrode separation (i.e. $h = 0$) and an infinite target radius. Comparison of predictions to experimental results will be presented in the next section.

It is clear from equation (15) that when targets of equal diameter are used there should be no distribution in film composition. In fact, for the case of two equal diameter targets, equation (15) reduces to

$$\text{vol. \% } j = \frac{\Gamma_j}{\sum_{i=1}^{N} \Gamma_i} \tag{16}$$

Computer calculated plots of equation (15) are shown in Figure 3 which demonstrates that large lateral gradients in film composition may be obtained by varying the relative ratios of target radii and target sputtering rates. Further variation in deposited film composition gradients could be obtained by varying the radial distance of each target from the rotation axis, the effective target radius which is exposed to the discharge, and the target to substrate separation.

III. EXPERIMENTAL RESULTS

In order to test the equations derived in section II, films were grown under a wide variety of deposition conditions using a multi-target RF sputtering system which is turbomolecular pumped and can accommodate up to four targets. The diameter of each target exposed to the plasma can be adjusted by means of grounded guard rings. Each target

may be empowered separately, sequentially, or simultaneously while the substrate platen is either stationary or rotating at a variable rate. The substrates may be heated, cooled, and/or biased. Further details on the sputtering system are contained in reference 17.

The thickness distributions of films deposited by decoupled plasma multitarget sputtering were determined experimentally by β-backscattering. In this technique, a β-particle beam impinges on a predetermined area of the sample surface and the intensity of the backscattered flux over a given solid angle is sampled using a Geiger tube and counter. A Pm^{147} source which has a maximum emission energy of 0.23 MeV was used in these experiments. The lower energy β-particles were removed from the beam by placing a 4.69 mg/cm^2 aluminum absorber between the sample and the β source. A schematic diagram of the apparatus is given in Figure 4. The measured intensity at the detector is a function of system geometry, film composition (through the average atomic mass number); film density, film thickness, and, if the film is thin, substrate material. In the present experiments all variables were held constant except film thickness. Figure 5 is a calibration plot of backscattered β intensity as a function of film thickness for InSb films deposited on glass substrates. InSb film thicknesses were determined by Tolanski interferometry and are accurate to within $\pm$ 10%. It was found that the calibration curve in Figure 5 was independent of applied target bias and Ar sputtering pressure over the entire range used in the following experiments: 500 V $\leq$ V $\leq$ 1500 V and 1 mTorr $\leq$ P $\leq$ 35 mTorr.

In order to determine $F(x,y)$, the stationary film thickness distribution, InSb films were deposited in separate runs on 20 cm diameter glass substrates aligned such that their center was directly beneath the center of the target. All films were grown at ambient temperature with no applied substrate bias. The effective target diameter in all cases was 8.5 cm as defined by a grounded guard ring. Figure 6 shows a series of normalized thickness distributions from films grown on stationary substrates at $V = 1000$ V and Ar pressures of 1, 15, and 35 mTorr. The electrode separation was 3.9 cm. The data points are measured values while the solid line is the distribution predicted from von Hipple's equation (20) for a disc target. The absolute magnitude of film thickness increased with Ar pressure as expected, and the fit of the normalized curves to von Hipple's theory remained quite good in all cases. A similar agreement was obtained when V was varied from 500 to 1500 V at $P = 15$ mTorr.

The distribution of film thickness along the x' axis deposited from one target on a substrate rotating at 3 rev/min is shown in Figure 7. The sputtering conditions were $V = 1000$ V and $P = 15$ mTorr. The solid line shown in Figure 7 was calculated from equation (12) while the data points were determined by β backscattering. As can be seen, the agreement is quite good. The maximum in the film thickness distribution is shifted towards the center of rotation due to the velocity (i.e. time in plasma) dependence on the rotation radius vector ξ. Figure 8 shows both theoretical and measured distribution profiles along the y' axis. The profiles were found to be symmetric and very flat over a central region

with some fall off at large radii due to path length differences. The normalized measured film thickness distributions were not dependent on rotation rate within the limits of our machine (0.7 rev/min to 10 rev/min) or on deposition rate over the range of target voltage and Ar pressure investigated.

The sputtering rate at the target, Γ, can be determined from Figure 9 in which the measured deposition rate is plotted as a function of $s^2/(s^2 + h^2)$ for various values of target bias. The sputtering rate at the target is defined as the deposition rate at zero target-substrate separation and can be determined for each target bias voltage and sputtering pressure by extrapolating the linear regions of the curves in Figure 9 to $[s^2/(h^2 + s^2)] = 1$ (i.e. h = 0). The dependence of Γ on a target bias voltage and sputtering pressure can be determined as shown in Figure 10. Once Γ is known, the deposition rate at any point in the system can be calculated if the target radius, target substrate separation, and the distribution function are known.

IV. DISCUSSION

The model presented in this paper for predicting deposited film thickness and chemical composition is quite general. Deviations of the stationary substrate film thickness distribution from the von Hipple equation caused by factors such as scattering of sputtered atoms in the discharge at high pressures, increased sputtering rate at the edge of unshielded targets (i.e. edge effects), or substrate heating and biasing

may be handled either analytically or empirically. We have found that gas scattering can be neglected for Ar pressures up to at least 35 mTorr and edge effects are not a problem for well shielded targets. However, Schwartz et al. [21] have proposed a model for calculating the change in film thickness distribution for unshielded targets and their derived function may be inserted directly into equations (4) and (12). The change in the deposition rate due to substrate bias has been treated by Cuomo et al. [22] and may be included in the present model by normalizing the expression they derive and including it as a product function in the rate term of equation (4). Deviations from von Hipple distributions can also be handled empirically by measuring the actual stationary substrate distribution, approximating it with a continuous function, transforming the function to the rotating coordinate system, and substituting the transformed distribution function $F_j(x',y',t)$ into equation (16).

In the derivation of the rotating substrate thickness distribution function it was implicitly assumed that: (1) substrate rotation does not affect the plasma discharge characteristics, (2) the sputtering rate at the jth target was independent of the discharge parameters at the ith target, and (3) the deposition rate of a given species was not a function of the instantaneous film surface composition (i.e. the sticking probabilities were constant). Assumption (1) is justified since it was established experimentally that substrate rotation within the range 0.7 rev/sec $< \omega < 10$ rev/sec had no measurable effect on target deposition rate and hence on discharge conditions. In order for the sputtering rate at each target to be independent of the discharge conditions at the other

targets as required by assumption (2), the power applied to each target must be independently controlled, the plasmas must be sufficiently separated such that there is no electrical interaction, and the targets must be shielded to prevent cross-contamination. Thus the rotation radius should be as large as possible. However, increasing ρ decreases η_j since the substrates are exposed to the targets for smaller fractions of the rotation period and some compromised is therefore required. In our system with ρ = 19 cm, no change in the stationary substrate deposition rate under one target was observed when the peak-to-peak RF voltage on a second target was varied between 0 and 1500 V.

The dependence of the deposition rate on substrate surface coverage becomes important for low deposition rates and short exposure times, i.e. times on the order of or less than that required to form a monolayer per target pass. In this case if there is a large difference in the sticking probability of different deposited species on the substrate or on each other, the deposition rate may exhibit a strong time dependence. However, if the sticking probabilities are known as a function of surface coverage, this effect can be accounted for in the model by intergrating equation (3) over the exposure time for point (x',y'). The terms $R_j(0,0)$ and $\eta_j(0,0)$ must be treated as time dependent and thus intergrated along with the transformed distribution function $F_j(x',y't)$.

The film thickness at (0,0) for stationary and rotating substrates differs by the factor $\eta_j(0,0)$ which was found to be independent of ω. However, it should be pointed out that the predicted value of $\eta_j(0,0)$ depends on the value of r_{oj} that is chosen. The predicted value of $\eta_j(0,0)$

in the absence of cross-contamination will be on the order of but slightly less than the measured value due to the truncation of the stationary distribution.

Plots of s and h versus deposition rate, such as those shown in Figure 9, can be used to determine values of Γ as a function of V and P. Γ is independent of system geometry and only a function of V and P. Therefore once $\Gamma(V,P)$ has been determined, the film thickness at any point in the substrate plane may be predicted as a function of deposition variables using the equations derived in section II.

The composition gradients shown in Figure 6 indicate that with decoupled plasma multitarget sputtering one can, as in cosputtering, deposit a complete thin film alloy system in a single run. However, in contrast with cosputtering, homogeneous films of any alloy composition as well as films with any desired lateral or depth compositional variation can be grown. For example, using two equal diameter binary targets, InSb and GaSb, we have grown $In_{1-x}Ga_xSb$ films at compositions ranging from $x = 0$ to $x = 1$ [16]. We have also grown layered structures with periods of 100 Å and less, and continuously graded chemical junctions [17]. Additional control over film chemistry can be obtained by varying the rotation radius, the target diameter exposed to the plasma, and the target-substrate separation. Doping can be accomplished using small diameter targets with low target bias and large target-substrate separations.

ACKNOWLEDGMENTS

The authors would like to acknowledge Mr. Jon Culton of the Coordinated Science Laboratory for the design and construction of the β-backscattering device.

References

1. J. L. Vossen, RCA Review 32, 289 (1971).

2. L. I. Mendelsohn, E. D. Orth, and R. E. Curran, J. Vac. Sci. Technol. 6, 363 (1969).

3. G. Muh, R. J. Wright, J. S. Chapin, and J. E. Fuller, Sputter Coating of TiC on Cutting Tools, Dow Chemical, Rocky Flats Div., publication RFP-1702, February 1972.

4. S. F. Vogel and I. C. Barlow, J. Vac. Sci. Technol. 10, 381 (1973).

5. J. R. Gavaler, M. A. Janocko, and C. K. Jones, J. Vac. Sci. Technol. 10, 17 (1973).

6. See for example, L. I. Maissel, Handbook of Thin Film Technology, edited by L. I. Maissel and R. Glang, McGraw-Hill, New York, 1970, p. 4-39.

7. W. R. Sinclair and F. G. Peters, Rev. Sci. Instr. 33, 744 (1962).

8. J. J. Hanak, LeVide 175, 11 (1975).

9. B. N. Chapman, D. Downer, and J. Guimaraes, J. Appl. Phys. 45, 2115 (1974).

10. G. K. Whener and D. J. Hajecek, J. Appl. Phys. 42, 1145 (1971).

11. A. D. G. Stewart and M. W. Thompson, J. Mater. Sci. 4, 56 (1969).

12. J. E. Greene, B. R. Natarajan, and F. Sequeda-Osorio, submitted for review to J. Appl. Phys.

13. J. J. Hanak, H. W. Lehmann, and R. K. Wehner, J. Appl. Phys. 43, 1666 (1972).

14. J. J. Hanak, J. Mater. Sci. 5, 964 (1970).

15. C. Corsi, J. Appl. Phys. 45, 3467 (1974).

16. J. E. Greene, C. E. Wickersham, and J. L. Zilko, 3rd International Conference on Thin Films, Budapest (August 1975), to be published in Thin Solid Films, May 1976.

17. J. E. Greene, C. E. Wickersham, and J. L. Zilko, to be published in J. Appl. Phys. June 1976.

18. J. E. Greene, C. E. Wickersham, J. L. Zilko, L. B. Welsh, and F. R. Szofran, J. Vac. Sci. Technol. Jan. 1976.

19. C. E. Wickersham, J. L. Zilko, and J. E. Greene, unpublished data.

20. A von Hipple, Ann. Physik. 81, 1043 (1926).

21. G. C. Schwartz, R. E. Jones, and L. I. Maissel, J. Vac. Sci. Technol. 6, 351 (1969).

22. J. J. Cuomo, R. J. Gambino, and R. Rosenberg, J. Vac. Sci. Technol. 11, 34 (1974).

23. J. E. Greene and C. E. Wickersham, submitted for review to J. Appl. Phys.

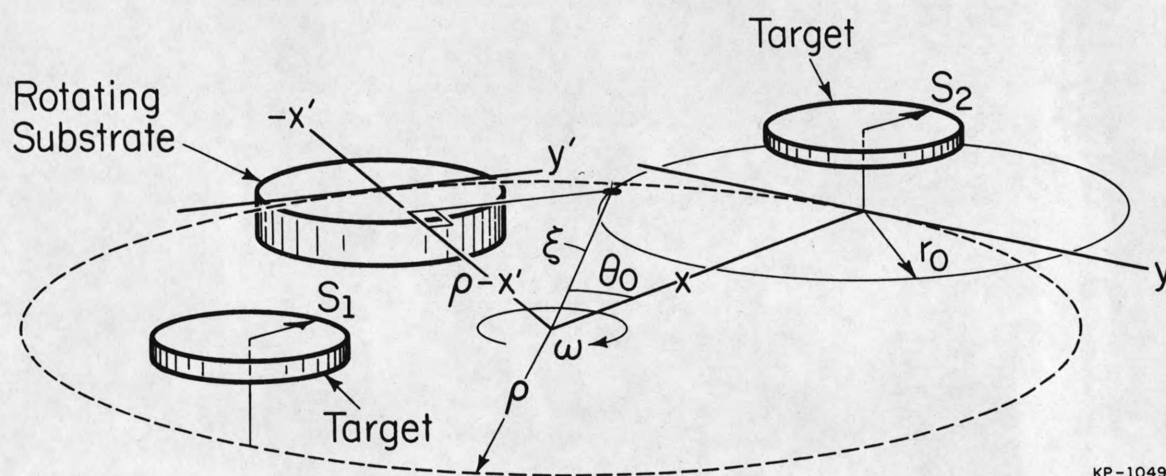

Figure 1. A schematic diagram defining the geometric relationship between the target and the rotating substrate in a multitarget RF sputtering system.

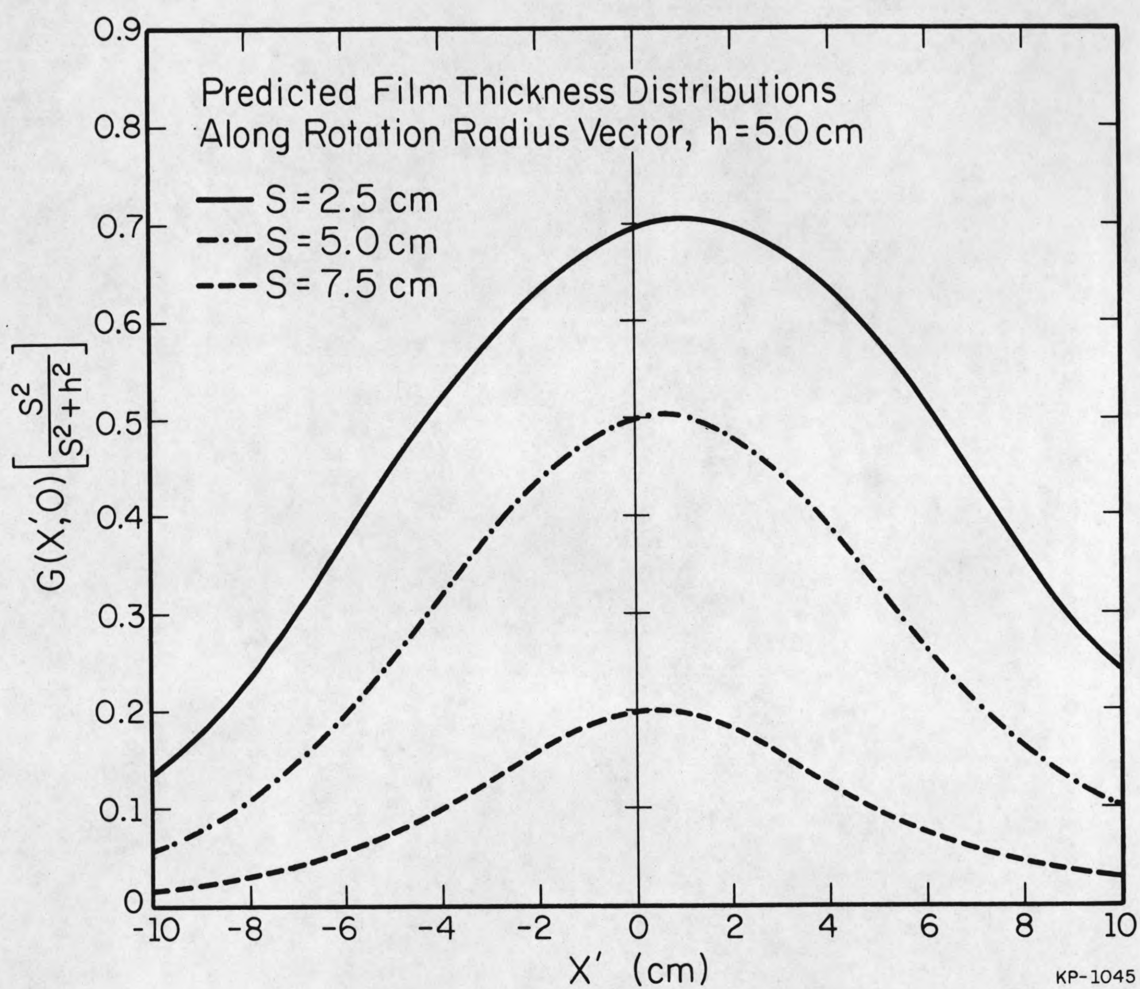

Figure 2. Theoretical thickness distributions for a rotating substrate with geometry given in Figure 1. In this case ρ = 20 cm, h = 5.0 cm.

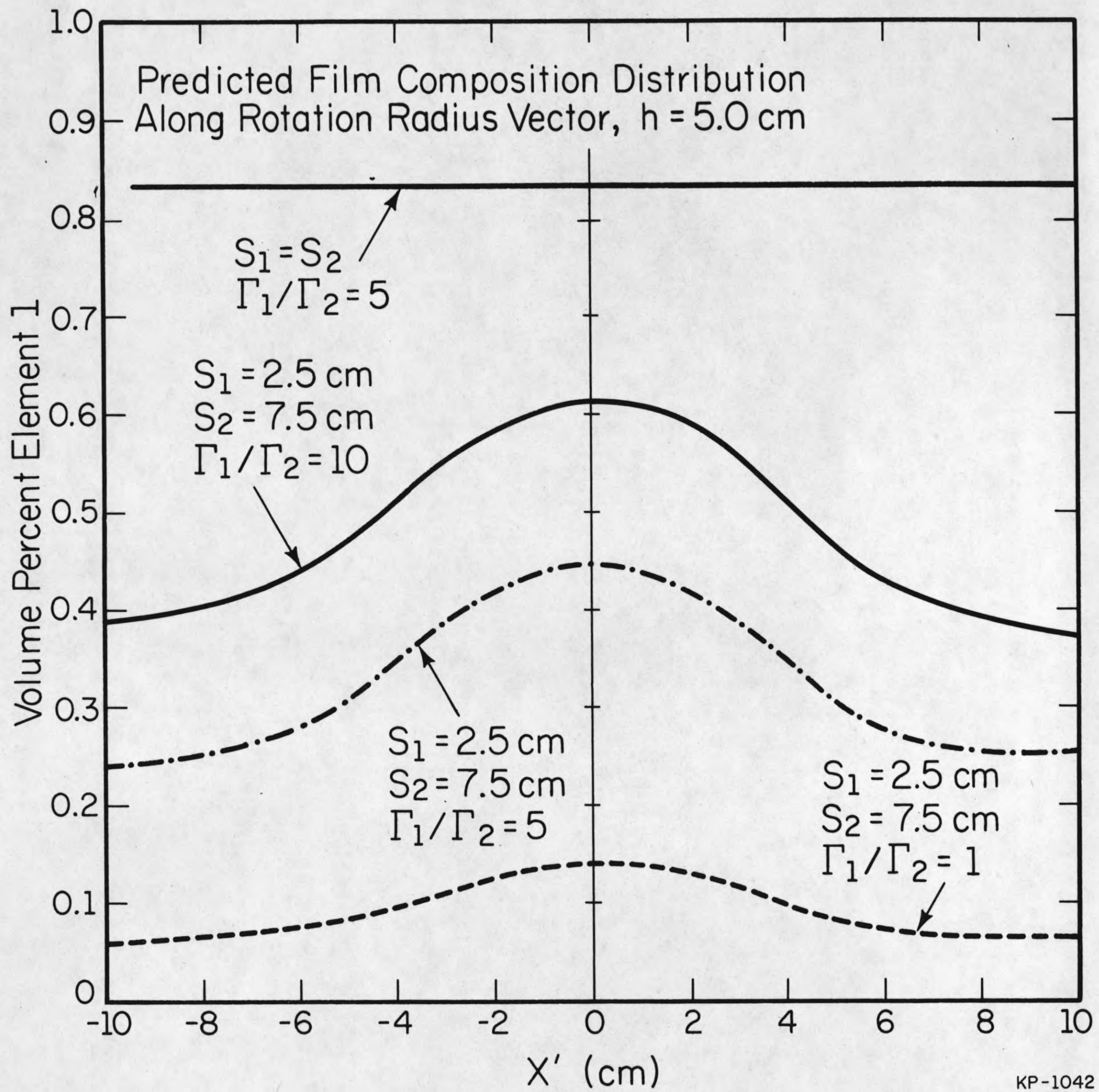

Figure 3. Theoretical composition distributions along the X' axis for a rotating substrate with ρ = 20 cm, h = 5.0 cm.

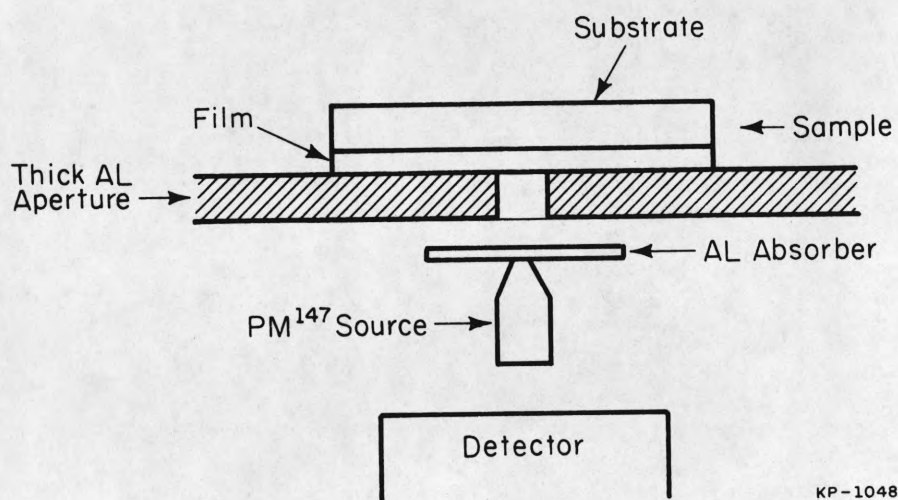

Figure 4. A schematic diagram of the β-backscattering apparatus used to measure film thickness distributions.

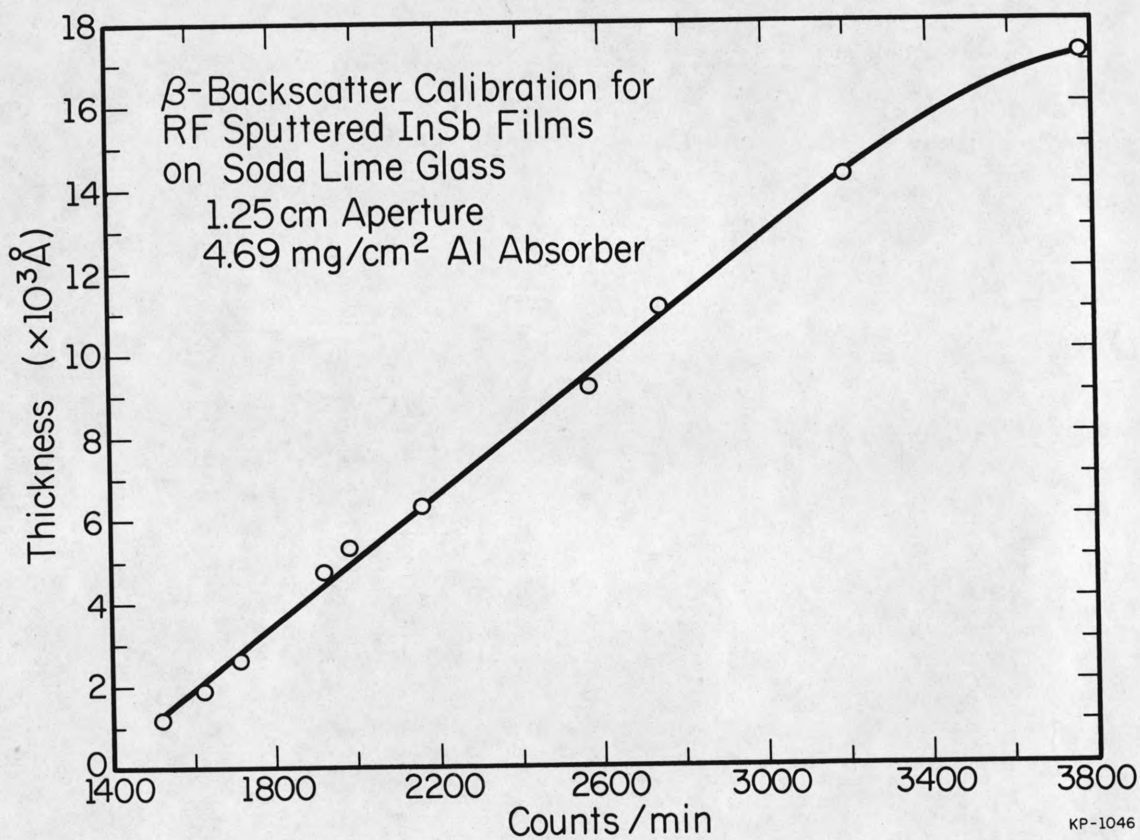

Figure 5. A calibration plot of β backscattering intensity vs. InSb film thickness measured interferometrically.

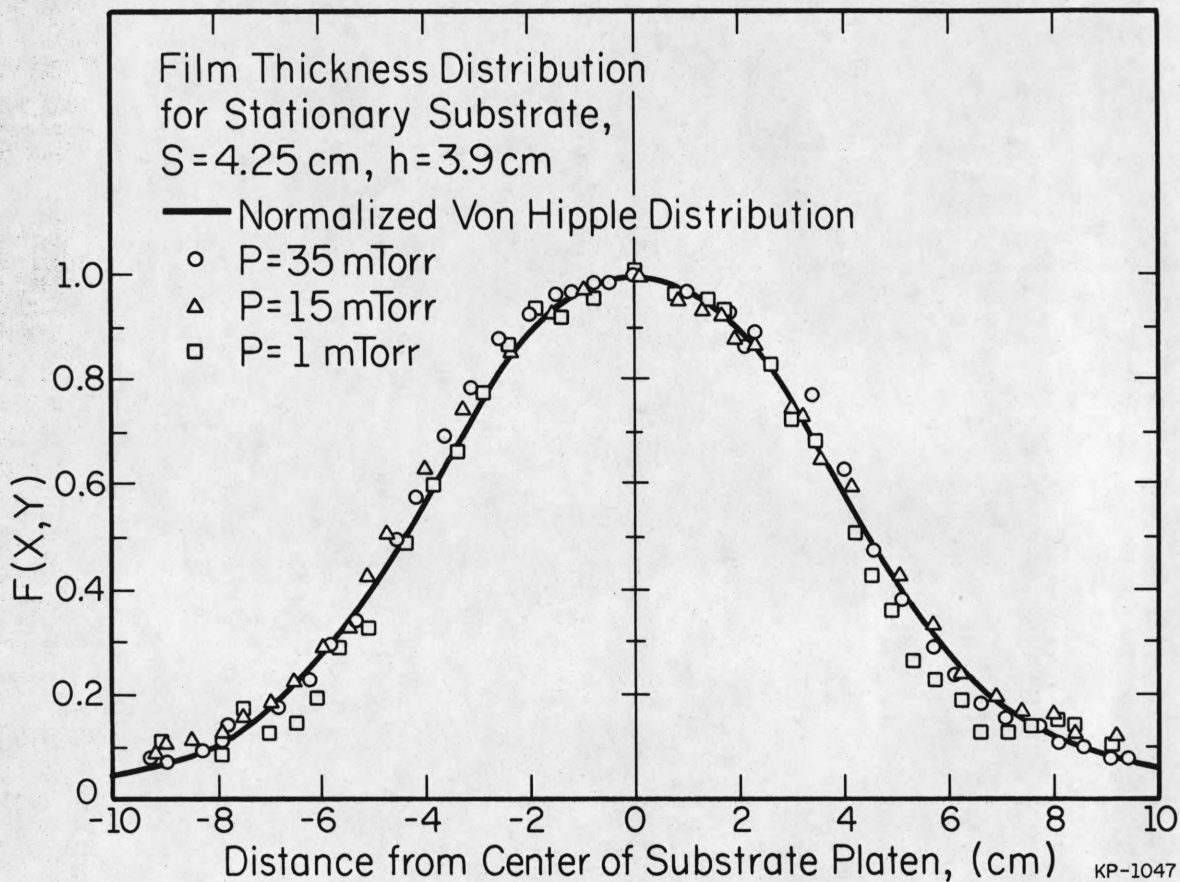

Figure 6. Stationary substrate thickness distributions for RF sputter deposited InSb at Ar sputtering pressures of 1, 15, and 35 m Torr.

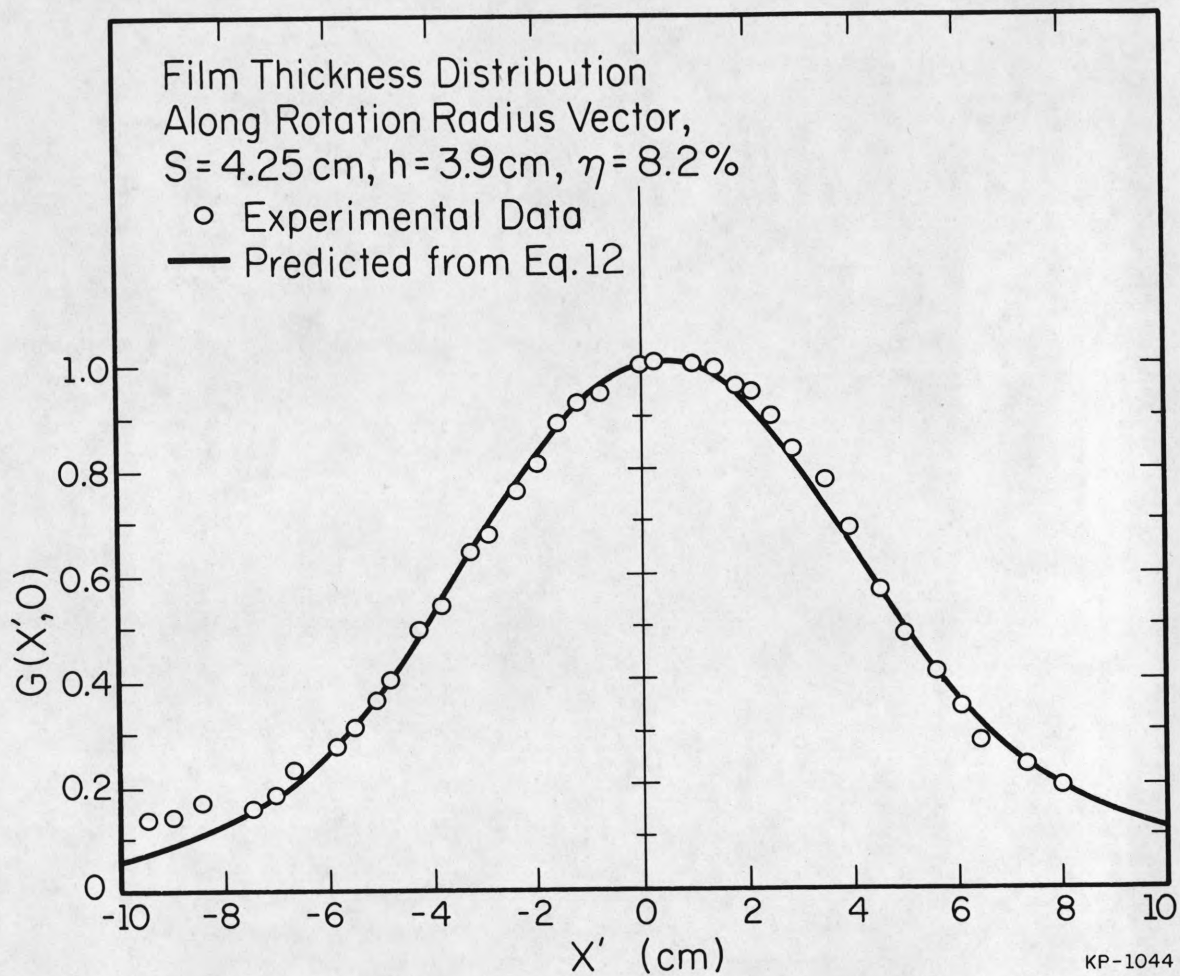

Figure 7. Rotating substrate thickness distribution along the X' axis for RF sputter deposited InSb. The film was deposited at V = 1000 V, p = 15 mTorr, ω = 3 rev/min, and h = 3.9 cm.

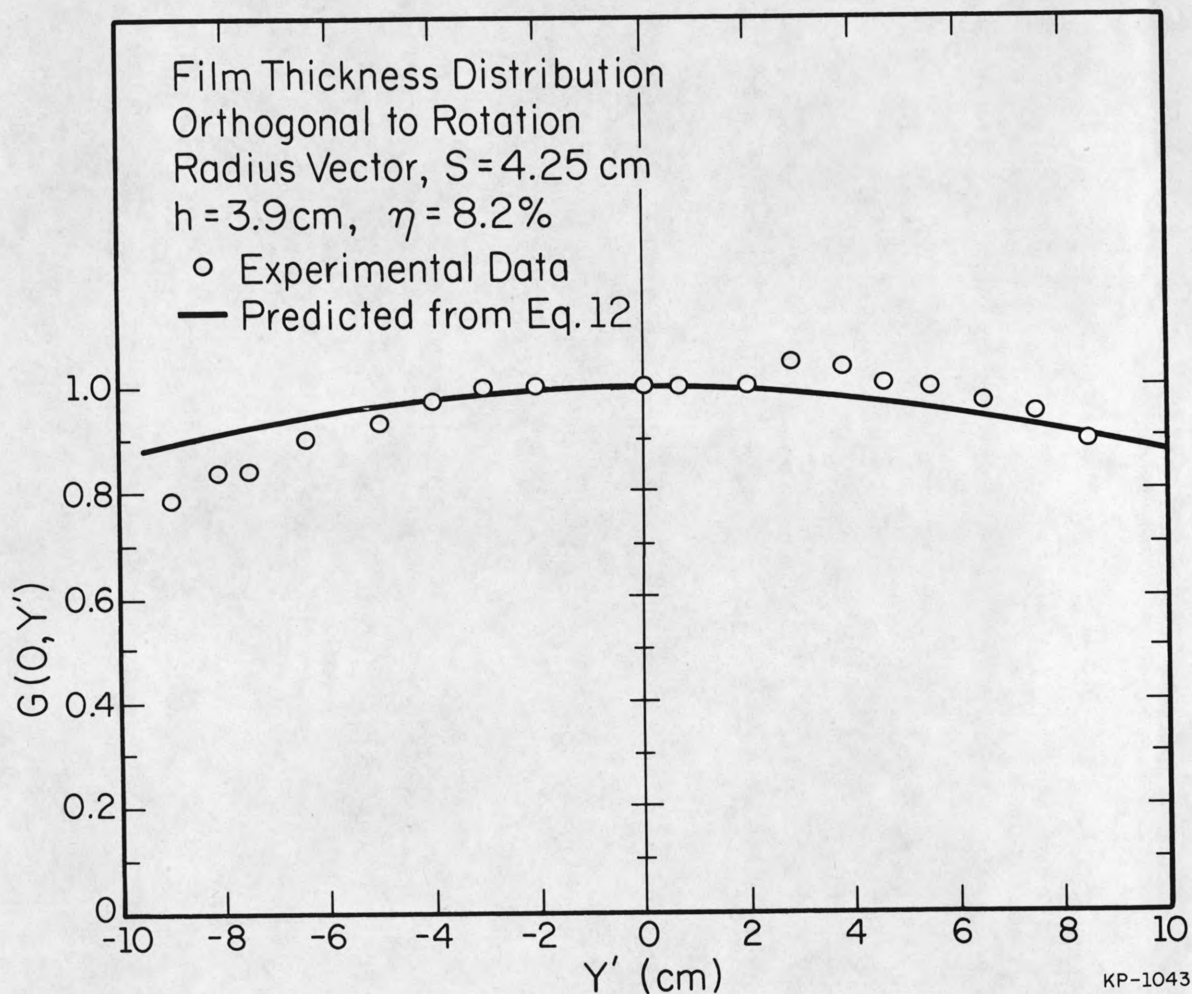

Figure 8. Rotating substrate thickness distribution along the Y' axis for RF sputter deposited InSb. The film was deposited with V = 1000 V, p = 15 mTorr, ω = 3 rev/min, and h = 3.9 cm.

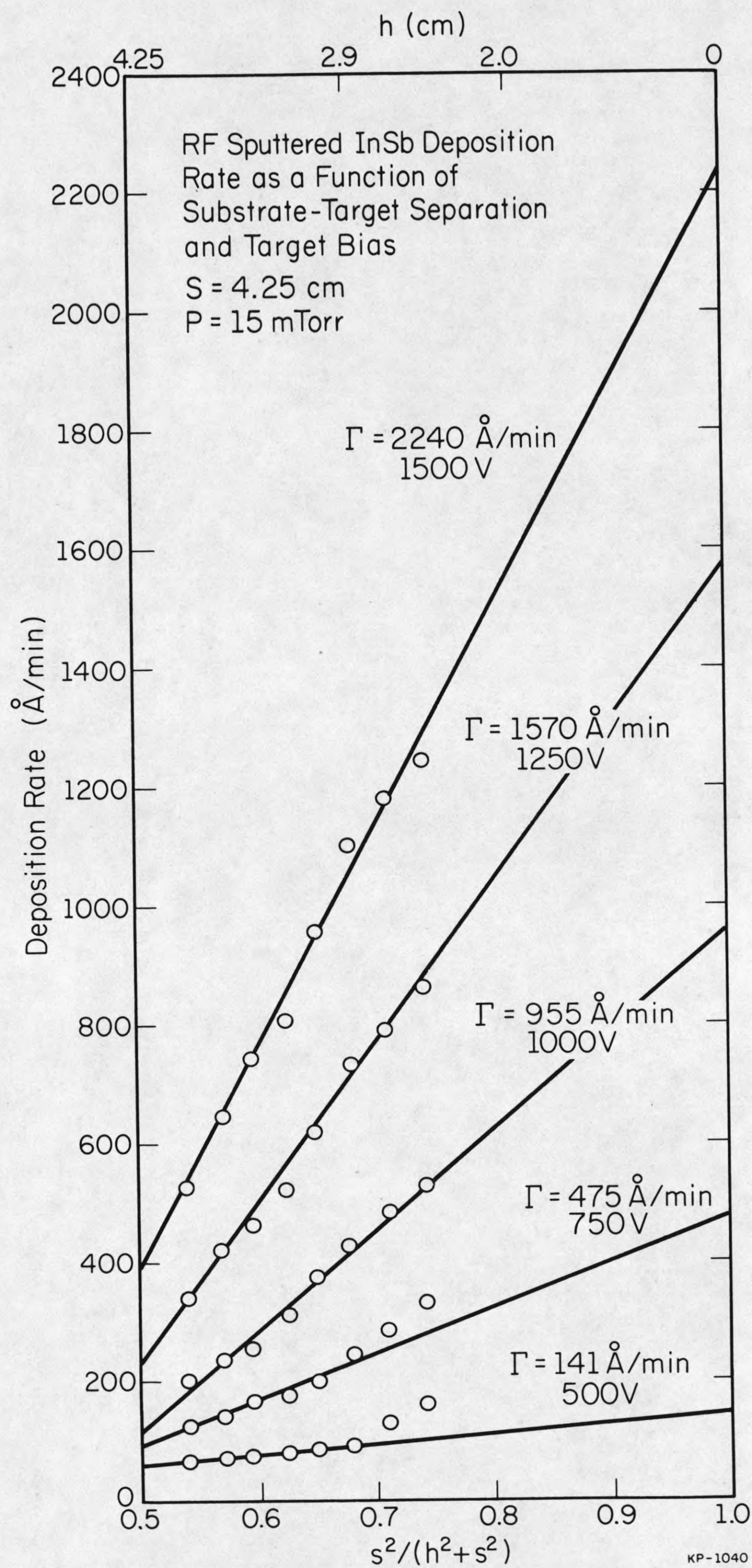

Figure 9. A plot of the deposition rate of RF sputtered InSb as a function of target-substrate separation.

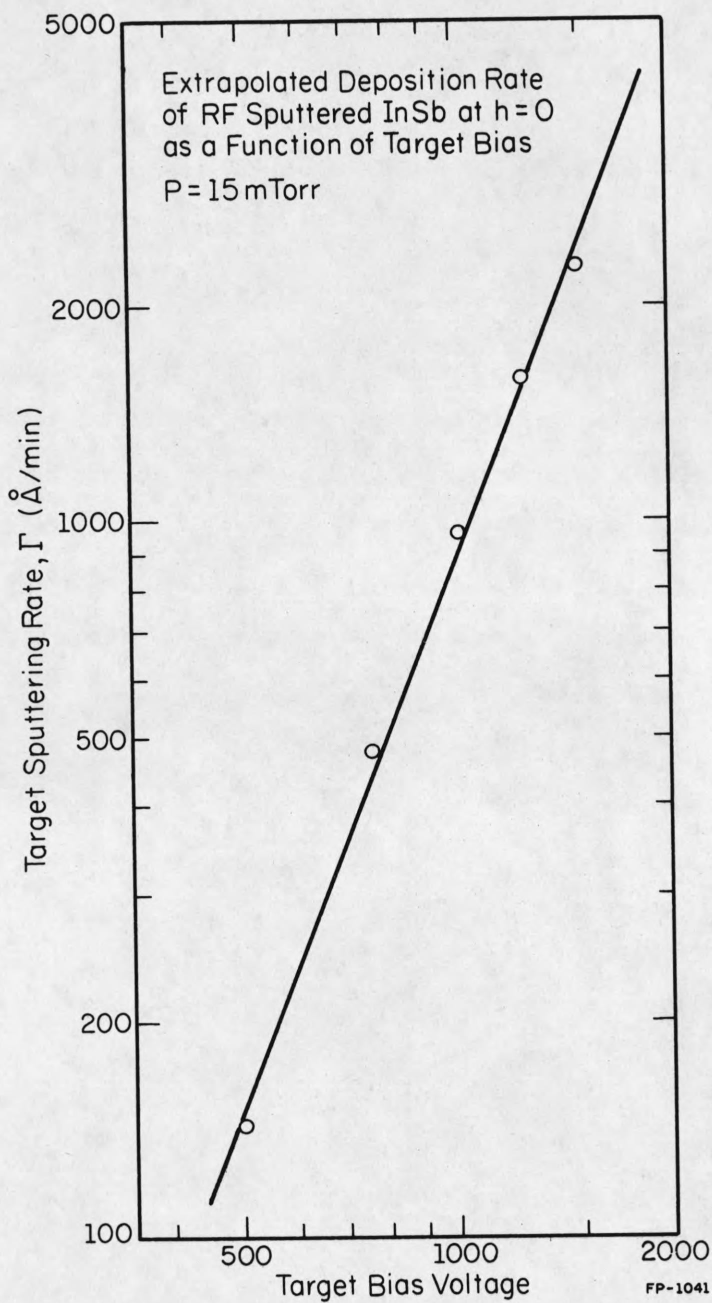

Figure 10. Extrapolated InSb sputtering rate as a function of target bias at an Ar pressure of 15 mTorr.